Molecular Neurobiology (2020) 57:1245–1258
https://doi.org/10.1007/s12035-019-01792-6

Serum Exosome MicroRNAs Predict Multiple Sclerosis Disease Activity after Fingolimod Treatment

Saeideh Ebrahimkhani[1,2,3] · Heidi N. Beadnall[2,3,4] · Chenyu Wang[2] · Catherine M. Suter[5,6] · Michael H. Barnett[2,3,4] · Michael E. Buckland[1,2,3] · Fatemeh Vafaee[7]

Received: 15 May 2019 / Accepted: 22 September 2019 / Published online: 12 November 2019

Abstract

We and others have previously demonstrated the potential for circulating exosome microRNAs to aid in disease diagnosis. In this study, we sought the possible utility of serum exosome microRNAs as biomarkers for disease activity in multiple sclerosis patients in response to fingolimod therapy. We studied patients with relapsing-remitting multiple sclerosis prior to and 6 months after treatment with fingolimod. Disease activity was determined using gadolinium-enhanced magnetic resonance imaging. Serum exosome microRNAs were profiled using next-generation sequencing. Data were analysed using univariate/multivariate modelling and machine learning to determine microRNA signatures with predictive utility. Accordingly, we identified 15 individual miRNAs that were differentially expressed in serum exosomes from post-treatment patients with active versus quiescent disease. The targets of these microRNAs clustered in ontologies related to the immune and nervous systems and signal transduction. While the power of individual microRNAs to predict disease status post-fingolimod was modest (average 77%, range 65 to 91%), several combinations of 2 or 3 miRNAs were able to distinguish active from quiescent disease with greater than 90% accuracy. Further stratification of patients identified additional microRNAs associated with stable remission, and a positive response to fingolimod in patients with active disease prior to treatment. Overall, these data underscore the value of serum exosome microRNA signatures as non-invasive biomarkers of disease in multiple sclerosis and suggest they may be used to predict response to fingolimod in future clinical practice. Additionally, these data suggest that fingolimod may have mechanisms of action beyond its known functions.

Keywords Multiple sclerosis · Gene expression · Exosome microRNAs · Fingolimod · Biomarker

Saeideh Ebrahimkhani and Heidi N. Beadnall are equal authorship contribution.
Michael E. Buckland and Fatemeh Vafaee are equal authorship contribution.

✉ Fatemeh Vafaee
f.vafaee@unsw.edu.au

Saeideh Ebrahimkhani
sebr0530@uni.sydney.edu.au

Heidi N. Beadnall
heidi@sydneyneurology.com.au

Chenyu Wang
chenyu.wang@sydney.edu.au

Catherine M. Suter
cathsuter@outlook.com

Michael H. Barnett
michael@sydneyneurology.com.au

Michael E. Buckland
michael.buckland@sydney.edu.au

[1] Department of Neuropathology, Royal Prince Alfred Hospital, Camperdown, NSW, Australia

[2] Brain and Mind Centre, University of Sydney, Camperdown, NSW, Australia

[3] Sydney Medical School, University of Sydney, Camperdown, NSW, Australia

[4] Department of Neurology, Royal Prince Alfred Hospital, Camperdown, NSW, Australia

[5] Division of Molecular Structural and Computational Biology, Victor Chang Cardiac Research Institute, Darlinghurst, NSW, Australia

[6] Faculty of Medicine, University of New South Wales (UNSW Sydney), Kensington, NSW, Australia

[7] School of Biotechnology and Biomolecular Sciences, University of New South Wales (UNSW Sydney), 2106, L2 West, Bioscience South E26, UNSW, Sydney, NSW 2052, Australia

Introduction

The majority of patients diagnosed with multiple sclerosis (MS) will have a relapsing-remitting course of disease (RRMS) that can vary significantly between individuals [1, 2]. Monitoring of disease activity is largely achieved via self-reporting, and composite surveillance including clinical examination and neuroimaging. Assessing the efficacy of any therapeutic agent in RRMS is similarly complex and costly. In recent years, a wider range of disease-modifying therapies to treat relapsing MS have become available [3, 4]. Fingolimod (marketed as Gilenya®) is a structural analog of sphingosine 1-phosphate (S1P) that acts as a S1P receptor modulator preventing lymphocyte egress from lymph nodes and was the first oral treatment approved for RRMS in 2010 [5–7]. There is currently no definitive blood test that would simplify the management of MS, in terms of reliably indicating disease activity and/or treatment response. However, recent research implicates circulating nanoparticles, called exosomes, as promising candidates.

Exosomes are small (~ 100 nm) membrane-bound vesicles that are constitutively released from seemingly all cells in the body; they contain a complex molecular cargo of proteins and nucleic acids from the cell of origin. Exosomes are thus components of all biological fluids, and exosomes secreted from many different tissues can be found in the peripheral circulation. Exosome biogenesis and secretion is tightly regulated, but in pathological states such as inflammation or neoplasia, exosome release appears upregulated. Remarkably, exosomes can also traverse the blood-brain barrier, raising the possibility that exosomes in the peripheral circulation may carry a signature of CNS pathology.

Exosomes are typically rich in small non-coding RNA cargo, in particular the well-studied microRNA (miRNA). Previous studies of MS have demonstrated miRNA dysregulation in multiple immune cell types, as well as whole plasma/serum, and cerebrospinal fluid [8–15]. We have previously found that purified exosomes from MS patients' sera also carry aberrant miRNA profiles, and that these are influenced by MS disease stage [8]. Whether serum exosome miRNA profiles are altered with disease activity and in response to successful pharmacological treatment of MS is currently unknown. Here, we have addressed these questions by studying the miRNA profiles of serum exosomes from patients with both active and quiescent RRMS prior to treatment with fingolimod and 6 months following. Machine learning techniques were applied to exosome miRNA data to identify miRNA signatures that are predictive of disease activity, and to reveal critical miRNAs involved in MS response to an immunomodulatory therapy. Integrative bioinformatics were used to uncover the potential functions of the identified miRNAs, providing a better understanding of MS immunopathogenesis and the action and metabolism of a successful pharmacological treatment.

Patients and Methods

Study Population and Clinical Characterization

RRMS patients naïve to fingolimod were recruited from the Royal Prince Alfred Hospital MS Clinic at the Brain and Mind Centre, University of Sydney, Australia. Criteria for inclusion were a diagnosis of relapsing-remitting MS (2010 McDonald criteria)[16], age between 18 and 60 years, and an expanded disability status scale (EDSS) score [17] of less than 6.5. Exclusion criteria were previous cladribine, fludarabine, or alemtuzumab; previous total body irradiation; immunosuppressant agents within the last 6 months; steroids, interferon-beta, glatiramer acetate, or any other concomitant immunomodulatory agent in the previous 30 days. Written informed consent was obtained from each patient. Ethical approval for the study was obtained from the University of Sydney Human Research Ethics Committee (2014/054).

All patients were clinically assessed by a neurologist (HNB, MHB) prior to commencement of fingolimod, and then at 6 and 12 months following. Demographic and MS disease-related data was documented at baseline and follow-up, and included clinical relapse information and EDSS scores. Brain magnetic resonance imaging (MRI) was performed using the same 3T General Electric MR750 scanner and the same acquisition protocol at all time points for all patients. The post-gadolinium T1-weighted sequence (T1) was used to assess the presence or absence of gadolinium (Gd) enhancing lesions, and this data was subsequently used to determine the presence or absence of disease activity [18–21]. Whole blood was collected from each patient at the same visit, at baseline and at 6 months. Blood was processed immediately by centrifugation and serum stored for exosome purification.

Exosome Purification and MicroRNA Profiling

Serum (1 mL from each individual) was treated with RNaseA to remove any non-exosomal RNA in the serum prior to exosome isolation by size exclusion chromatography, as previously described [8]; exosome purity and quantity were characterized and validated by nanoparticle tracking analysis, transmission electron microscopy, and western blotting as per international guidelines [22]; the adopted procedure is detailed in our former work [8]. RNA was isolated from purified and validated exosomes using the Plasma/Serum Circulating & Exosomal RNA Purification Kit (Norgen Biotek) and quality controlled for typical exosomal RNA profile with an Agilent 2100 Bioanalyser on a Eukaryote Total RNA chip. Barcoded sequencing libraries were prepared from the RNA as previously described [8]. Libraries were pooled and sequenced on an Illumina HiSeq 2000 System.

Table 1 Patient demographics

Characteristic	Value
Number of patients	29
Gender, male/female (%)	12/17 (41/59)
Average age at diagnosis, years ± SD	33.7 ± 9.9
Average disease duration, years (range)	4.9 (0.1–26.5)
Average age at study baseline, years ± SD	38.6 ± 10.2
Active disease at baseline[a], *n* (%)	14 (48)
Active disease at 6 months[a], *n* (%)	8 (28)
Average EDSS at baseline ± SD	1.7 ± 1.3
Average EDSS at 6 months ± SD	1.4 ± 1.3

SD standard deviation, *EDSS* expanded disability status scale

[a] Determined by presence of Gd-enhancing lesions on MRI

Data Pre-Processing and Differential Expression Analysis

Data pre-processing was performed using a pipeline comprising of adapter trimming (cutadapt), followed by genome alignment to human genome hg 19 using Bowtie (18 bp seed, 1 error in seed, quality score sum of mismatches < 70). Where multiple best strata alignments existed, tags were randomly assigned to one of those coordinates. Tags were annotated against mirBase 20 and filtered for at most one base error within the tag. Counts for each miRNA were tabulated and adjusted to counts per million miRNAs passing the mismatch filter. All samples achieved miRNA read counts > 45,000; miRNAs with low abundance (< 50 rpm across more than 20% of samples) were removed.

Normalization and differential expression analysis were performed using RNA-seq analysis tools in the Bioconductor "limma" package. Read counts were first converted to log2-counts-per-millions to stabilize variances at high counts. The mean-variance relationship was then estimated at the individual observation level [23] to adjust for different count sizes across samples and combined with sample-specific quality weights to down-weight outlier samples [24]. The transformed read counts were then entered into the standard limma empirical Bayes method pipeline for differential expression analysis estimating moderated t-statistics and the corresponding *p* values [25]. In any comparison, differentially expressed miRNAs were identified as those whose *p* value was < 0.05 with fold change doubled in either direction (i.e., $|\log2(\text{fold change})| \geq 1$).

Univariate and Multivariate Modelling

Logistic regression (LR) was used to identify linear predictive models with each miRNA as the univariate predictor. The quality of each model was depicted by the corresponding receiver operator characteristic (ROC) curve, which plots the true positive rate (i.e., sensitivity) against the false-positive rate (i.e., 1-specificity). The area under the ROC curve (AUC) was computed and 95% confidence intervals estimated using the method of Delong [26]. ROC curves were smoothed using Tukey's method for presentation [27]. The predictive power of combinations of multiple miRNAs as multivariate signatures of MS activity was assessed using Random Forest (RF) modelling [28]. We used out-of-bag (OOB) error as an

Table 2 MicroRNAs with significant expression differences between active and quiescent RRMS patients after 6 months of fingolimod treatment[a]

MicroRNA	Log_2 FC	Average expression[b]	*p* value	AUC (95% CI)
1246	2.137	4.855	0.00003	0.911 (0.789 1)
379-5p	1.417	8.887	0.00063	0.813 (0.628 0.997)
134-5p	1.28	8.926	0.00084	0.786 (0.594 0.977)
370-3p	1.335	8.347	0.00106	0.786 (0.596 0.976)
382-5p	1.297	9.333	0.00233	0.777 (0.576 0.978)
493-3p	1.205	6.497	0.00234	0.759 (0.55 0.968)
432-5p	1.387	8.777	0.00241	0.768 (0.57 0.966)
375	1.213	5.692	0.00315	0.768 (0.567 0.968)
485-5p	1.044	5.689	0.00453	0.786 (0.589 0.982)
411-5p	1.047	6.577	0.00809	0.723 (0.502 0.944)
323b-3p	1.029	8.126	0.00921	0.741 (0.508 0.974)
889-3p	1.033	6.727	0.01083	0.759 (0.484 1)
19b-3p	−1.052	7.464	0.0212	0.768 (0.567 0.969)
122-5p	1.01	12.679	0.0242	0.652 (0.406 0.898)
127-3p	1.017	7.894	0.02438	0.759 (0.558 0.96)

FC fold change, *AUC* area under the ROC curve, *CI* confidence interval

[a] Only miRNAs meeting the log2 FC threshold of > 1 are shown

[b] Log_2 reads per million

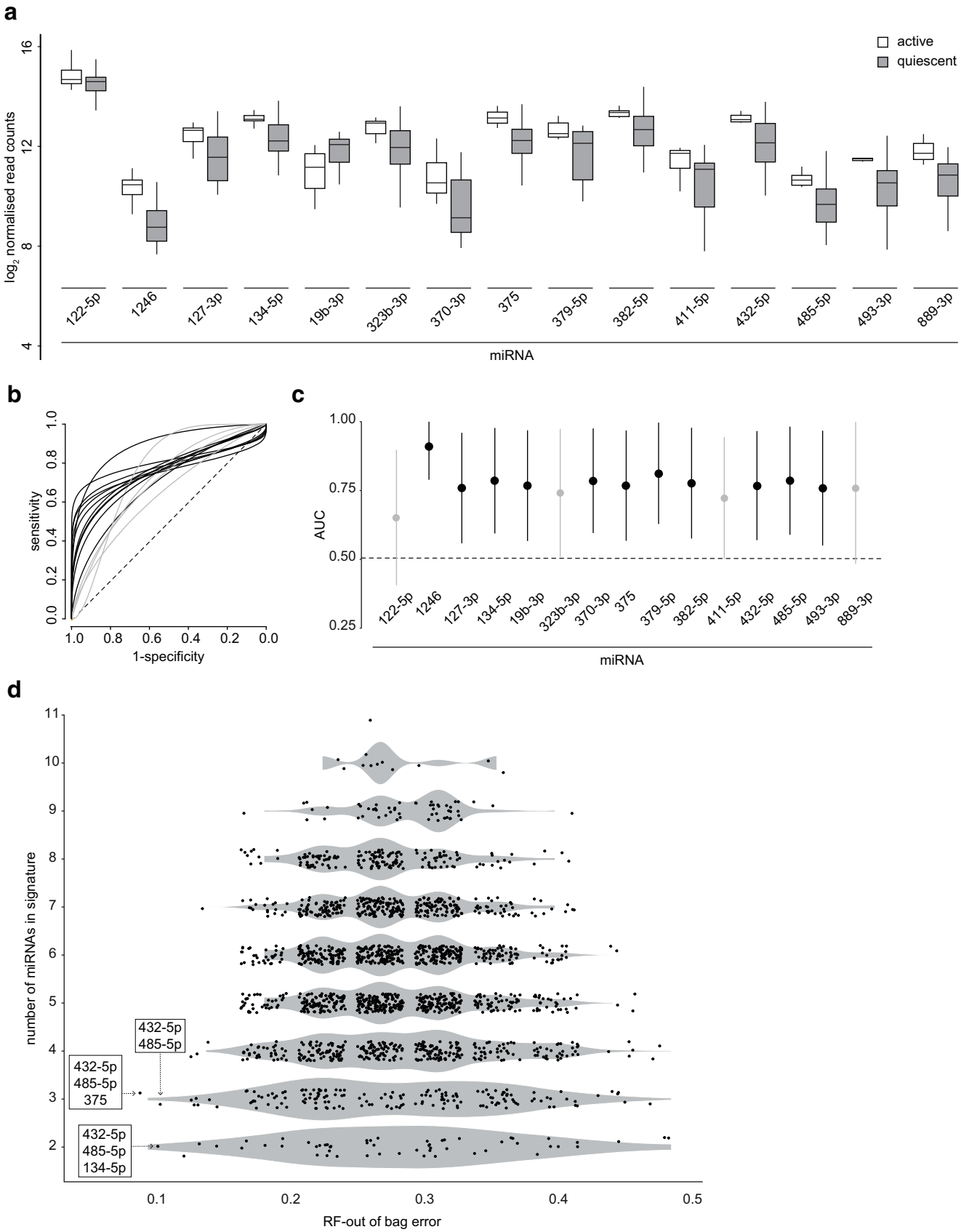
a
active
quiescent
log2 normalised read counts
16
12
8
4
122-5p
1246
127-3p
134-5p
19b-3p
323b-3p
370-3p
375
379-5p
382-5p
411-5p
432-5p
485-5p
493-3p
889-3p
miRNA
b
sensitivity
1.0
0.8
0.6
0.4
0.2
0.0
1-specificity
c
AUC
1.00
0.75
0.50
0.25
miRNA
d
number of miRNAs in signature
11
10
9
8
7
6
5
4
3
2
432-5p
485-5p
432-5p
485-5p
375
432-5p
485-5p
134-5p
0.1
0.2
0.3
0.4
0.5
RF-out of bag error

◀ **Fig. 1** Exosomal miRNAs as markers of disease activity. **a** Box-and-whisker plots represents expression normalized values (i.e., log2-transformed reads-per-million) of exosomal miRNAs significantly altered in post-treatment active versus quiescent patients as determined by Bayes moderated *t* test with |log2 (fold change)| > 1 and *p* value < 0.05. **b** To examine the predictive power of each dysregulated miRNA, logistic regression and receiver operator characteristic (ROC) analysis was performed on individual miRNAs. Area under the ROC curve (AUC) was measured and the corresponding 95% confidence intervals were then computed for each miRNA. Eleven miRNAs with AUC confidence more than 0.5 were considered as statistically accurate univariate predictors of MS disease activity. **c** Random forest (RF) model was run using all possible combinations of those 11 miRNAs to assess whether signatures of multiple miRNAs would improve the predictive power as determined out-of-bag error rates of the corresponding multivariate RF models. A combination of two or three miRNAs provided a predictive power of 92% for disease activity

unbiased estimate of the validation set prediction error as implemented by the R "randomForest" package.

Functional Predictions and Enrichment Analysis of MS-Associated MicroRNAs

Pathway and gene ontology enrichment analysis was performed on targets of the identified exosomal miRNAs. Molecular Signatures Database (MSigDB) [29], version 6.1, was used to retrieve KEGG pathways (186 pathways on 12,875 genes), Reactome pathways (674 pathways on 37,601 genes), and gene ontology (GO) biological processes (4436 GO terms on 506,182 genes). Human miRNA targets were retrieved from publicly available datasets of experimentally validated and predicted datasets using *multiMiR* v2.2 [30]. MultiMiR is a miRNA-target interaction R package and database which compiles nearly 50 million records in humans and mice from 11 different databases. Targets of miRNAs under study were included if experimentally validated or predicted by at least two databases. Pathway enrichment analysis of targets was achieved using the right-sided Fisher's exact test. Nominal *p* values were adjusted for multiple hypothesis tests using Benjamini and Hochberg (FDR) correction.

Similarly, miRNA enrichment analysis was performed using the right-sided Fisher's exact test whose *p* value for the null hypothesis is computed based on the hypergeometric distribution:

$$p = \frac{1}{\binom{N}{n}} \sum_{i=k}^{i=n} \binom{n}{i} \binom{N-K}{n-i},$$

where N is the total number of target genes annotated in multiMiR, n is the number of all up/downregulated genes (in MS brain lesions, *c.f.* "Results"), K is the total number of genes targeted by the miRNA as annotated in multiMiR, and k is the number of target genes inversely regulated by the miRNA of interest—i.e., total number of downregulated genes targeted by an upregulated miRNA or vice versa; inverse regulation was considered to capture miRNA primary function of *gene silencing*. The nominal *p* values were adjusted for multiple hypothesis testing using Bonferroni correction. Enrichment analyses were implemented in R using "stats" packages.

Results

Patient Characteristics and Data Pre-Processing

Twenty-nine RRMS patients, whose relevant demographics are shown in Table 1, were included in the study. An unbiased high-throughput sequencing on serum exosome miRNAs was performed, capturing the complete profile of miRNAs in patients' sera. Size exclusion chromatography was used for exosome isolation coupled with RNAse treatment of extracts to interrogate exosomal-associated miRNAs as a source of biomarkers distinct from free circulating miRNAs [8]. Transmission electron microscopy was adopted to represent close-up images of single exosomes and nanoparticle tracking analysis to provide an overview of size distribution and concentration of isolated exosomes. These analyses revealed a population of nanovesicles with a predominant size of 95 nm and cup-shaped morphology typical of exosomes. Western blotting confirmed that the isolated particles expressed characteristics of exosome markers. RNA extraction from each sample yielded the typical RNA profile for exosomes, with the absence ribosomal RNA and enrichment of small (< 200 nt) RNA species.

The expression profiles of exosomal miRNAs, as determined by deep sequencing, were analysed at two distinct time points, i.e., baseline, when the patients were treatment-naïve, and 6 months after the commencement of immunomodulatory therapy with fingolimod. A total of 1924 miRNAs were screened for each sample; all samples achieved miRNA read counts > 45,000. For each comparison, miRNAs with low abundance (< 50 read counts across more than 20% of samples) were removed, retaining around 11–12% of miRNAs in any comparison. Read counts were normalized to adjust for RNA and sample-level biases. There were no significant differences in age (using Mann–Whitney *U* non-parametric test) and gender (using Fisher's exact test) between any two groups compared in this study.

Serum Exosome MicroRNA Signatures in RRMS Before and After Fingolimod Treatment

We first sought a circulating exosome miRNA signature of disease activity in patients before they commenced fingolimod. At this baseline, differential expression analyses

a

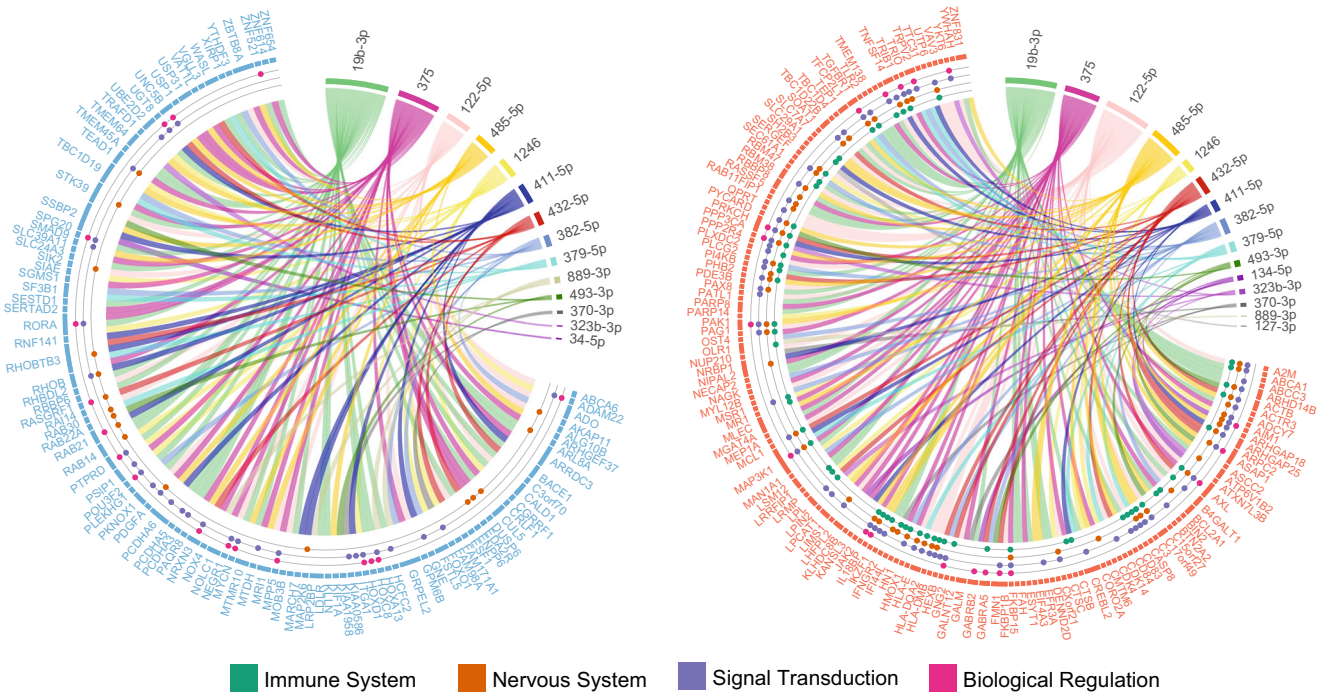

b

Immune System

Biological processes enriched by up-regulated genes

Immune system process (7.6E-23), Regulation of immune system process (1.0E-19), Regulation of innate immune response (1.5E-07), Defense response (2.0E-07), Regualation of cytokine production (3.6E-07), Phagocytosis (8.8E-07), Response to cytokine (9.3E-06), leukocyte activation (1.4E-03), Regulation of immune effector process (1.8E-03), lymphocyre activation (2.8E-03), Regulation of type I interferon production (3.6E-03), Immune system developmnet (4.1E-03), Regulation of chemokine production (5.4E-03), Cellular response to cytokine stimulus (6.0E-03), Cellular response to interferon-gamma (6.3E03), Positive regulation of interleukin 1-beta production (7.0E-03), Positive regulation of macrophage dervied foam cell differentiation (3.6E-04), Regulation of leukocyte proliferation (9.7E-03), Regulation of inflammatory response (9.4E-03), Wound healing (1.4E-10), Response to wounding (1.9E-10), Regulation of response to wounding (1.3E-04)

Nervous System

Biological processes enriched by up-regulated genes

Neurogensis (2.2E-03) and negative regulation of dendrite development (5.3E-03)

Biological processes enriched by down-regulated genes

Neurogenesis (3.0E-07), Neuron differentiation (3.0E-04), Peripheral nervous system develpment (8.2E-04), Ensheathment of neurons (3.3E-03), Peripheral neruvous system axon ensheathment (3.3E-04), Schwann cell development (6.7E-04) and Schwann cell differentiation (1.4E-03)

Signal Transduction

Biological processes enriched by up-regulated genes

Intracellular signal transduction (3.4E-13), Regulation of intracellular signal transduction (4.6E-09), Regulation of GTPase activity (3.7E-05), FC receptor signaling pathway (3.7E-05), Regulation of protein activation cascade (2.3E-04), Interferon-gamma mediated signaling pathway (2.3E-04), Enzyme linked receptor protein signaling pathway (4.0E-04), Ephrin receptor signaling pathway (7.4E-04), Transmemebrane receptor protein trosine kinase signaling pathwat (8.8E-04), Positive regulation of intracellular signal transduction (9.5E-04), Antigen receptor mediated signaling pathway (6.7E-03), Regulation of small GTPase mediatated signal.

Biological processes enriched by down-regulated genes

Intracellular signal transduction (1.8E-06), Regulation of intracellular signal transduction (3.09E-05) and small GTPase mediated signal transduction (8.08E-05)

Biological Regulation

Biological processes enriched by up-regulated genes

Regulation of cell differenctiation (4.3E-10), Positive regulation of gene expression (3.0E-06), Regulation of cell proliferation (6.7E-06), Regulation of cell morphogenesis involved in differentiation (2.5E-03), Negative regulation of cell communication (6.9E-03), Regulation of sequence specific DNA binding transcription factor activity (4.5E-04), Positive regulation of cell development (5.1E-04), Positive regulation of actin filament polymerization (7.2E-03), Regulation of cellular component movement (9.6E-03) and regulation of cell activation (2.2E-10)

Biological processes enriched by down-regulated genes

Regulation of transcription from RNA polymerase II promoter (3.4E-03), Biological adhesion (2.2E-04), Anatomical structure formation involved in morphogenesis (6.2E-03) and cell-cell adhision (7.9E-03).

revealed 12 miRNAs with significant differences ($p < 0.05$) between those patients with active ($n = 14$) versus quiescent ($n = 15$) disease. However, only two of these miRNAs, *miR-194-5p* ($p = 0.0065$, log fold change = 1.12) and *miR-374a-5p* ($p = 0.0131$, log fold change = 1.18), had changes in abundance that met the stringent thresholds ($\log_2$ fold change >

◀ **Fig. 2** Predicted functional role of miRNAs associated with MS disease activity. **a** The networks represent MS-associated miRNA-target interactions including miRNAs differentially expressed in active versus quiescent phases of MS and gene targets specific to disease activity in MS brain lesions; a public dataset (GSE108000) was used to identify genes significantly altered in chronic active versus inactive MS lesions of post-mortem brain tissues. Accordingly, 153 and 102 target genes identified to be upregulated (red, right) and downregulated (blue, left) whose interactions with miRNAs were visualized in separate networks to improve the readability. Target genes were used to perform functional enrichment analysis of biological processes. Enriched functions were categorized into four MS-relevant categories of biological processes, i.e., immune system, nervous system, signal transduction, and biological regulation. Targets were annotated with biological process categories if the gene had been annotated by at least one GO term within the associated category. **b** A list of overrepresented gene ontology biological processes is shown with the corresponding FDR values in parentheses

1). Six months after fingolimod treatment, the number of miRNAs with significant differences in abundance (log2 fold change > 1 and $p < 0.05$) increased to 15 (Table 2). Most of these miRNAs (14/15) were "positive" biomarkers of active RRMS: that is, their abundance was greater in patients with active disease (Fig. 1a). The increase in the number of differentially expressed miRNAs after treatment is reminiscent of a previous report of the effects of interferon-β on miRNA [9], where administration of medication elicited a reduction in within-group variation. We thus measured the variance in expression of each miRNA across samples within active and quiescent cohorts, both before and after treatment. The mean variance was reduced significantly in both quiescent and active patients after fingolimod compared to baseline ($p = 1.571e{-}05$ for quiescent, $p = 0.0207$ for active; Mann–Whitney *U* test). Accordingly, the heteroscedasticity of miRNA expression values was reduced with fingolimod therapy, improving statistical hypothesis testing (reducing type II error). Hence, further analyses were focused on the 15 miRNAs that differed between active and quiescent RRMS post-fingolimod treatment.

The predictive power of each miRNA was assessed using univariate logistic regression. Receiver operator characteristic (ROC) curves (generated by plotting the true positive rate against the false-positive rate; Fig. 1b) and subsequent measurement of the area under the ROC curve (AUC) revealed that four of the 15 miRNAs had 95% confidence intervals that overlapped that of a random prediction (Fig. 1c). The remaining 11 miRNAs (*miR-1246*, *-127-3p*, *-19b-3p*, *-134-5p*, *-370-3p*, *-375*, *-379-5p*, *-382-5p*, *-432-5p*, *-485-5p* and *-493-3p*) were considered as statistically accurate univariate predictors of MS activity, with ROC AUC ranging from 0.65 to 0.91. These miRNAs were considered suitable for assessment in multivariate analyses to ask whether combinations of miRNAs could improve accuracy.

Random forest (RF) modelling on all possible combinations of 11 miRNAs was performed, trialling a total of 2037 signatures comprising 2 to 11 miRNAs. Remarkably, the out-of-bag error rates indicated three combinations of only two miRNAs (*miR-432-5p* and *miR-485-5p*) or three miRNAs (*miR-432-5p*, *-485-5p*, *-375* and *miR-432-5p*, *−485-5p*, *−134-5p*) assigned individuals as having active or quiescent RRMS with > 90% accuracy (Fig. 1d). Including more than three miRNAs in the signature did not improve accuracy beyond 92%.

Functional Characterization of MicroRNAs Associated with MS Activity

Gene targets of miRNAs altered in active versus quiescent RRMS were retrieved from multiple miRNA-target interaction databases, and 4650 targets that are either experimentally validated or computationally predicted in at least two datasets were selected. To enhance the specificity of targets and subsequent functional analysis, a gene expression profile of post-mortem MS brain tissues derived from histopathologically defined active and inactive lesions [10] was obtained from NCBI GEO. Genes differentially expressed in chronic active versus inactive MS lesions were identified (i.e., $p < 0.05$ using limma moderated *t* test on normalized gene expression data retrieved from GSE108000) and overlapped on miRNA targets resulting in 153 upregulated and 102 downregulated target genes. These genes were considered as *MS-specific* targets of the identified exosomal miRNAs and underwent functional enrichment analysis for gene ontology biological processes. Overrepresented biological processes (FDR < 0.01) were summarized and stratified under four relevant categories of *immune system*, *nervous system*, *signal transduction* and *biological regulation* by consulting gene ontology hierarchy revealing multiple biological processes implicated in MS pathogenesis (*c.f.* "Discussion"). Networks of dysregulated miRNAs interacting with the target genes down- or upregulated in MS lesions are shown in Fig. 2a; targets were annotated with the biological processes detailed in Fig. 2b.

Tissue Specificity and Enrichment Analysis of MicroRNAs Associated with MS Activity

To investigate whether the altered regulations of the targets in brain lesions were likely triggered by the identified exosomal miRNAs, we sought to demonstrate if any of the miRNAs are predominantly regulated and thus packaged in brain, assuming that *brain-specific* miRNAs are more likely to target genes altered in MS brain lesions.

Accordingly, we used *human miRNA tissue atlas* [31] which reports the abundance of 1997 miRNAs in 61 tissue biopsies of different organs collected post-mortem from two male bodies. The database utilized a *tissue specificity index* (TSI), a quantitative, graded scalar measure for the specificity of expression of a miRNA with respect to different organs.

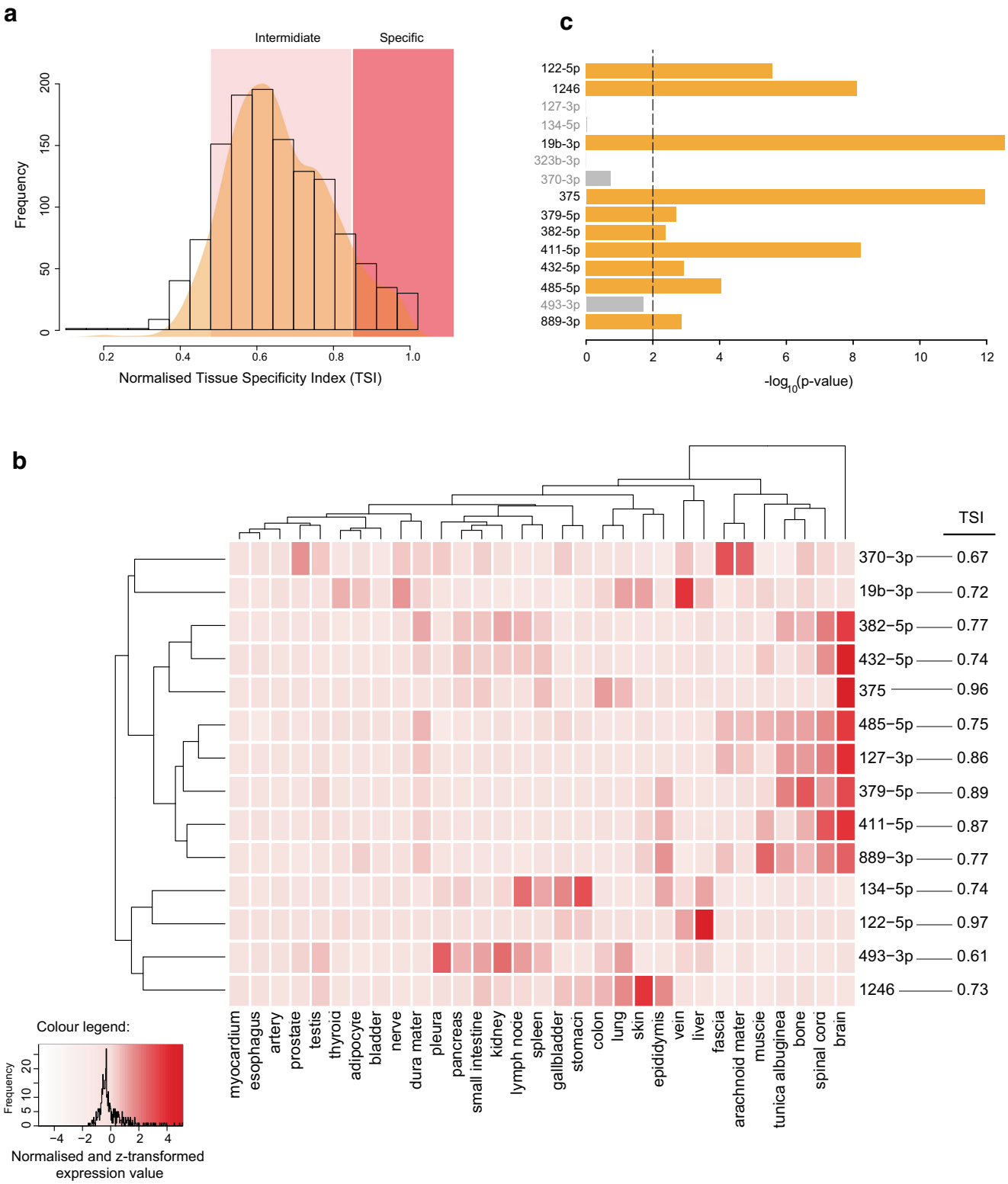

Fig. 3 Tissue specificity and enrichment analysis of miRNAs associated with MS disease activity. **a** The histogram shows the distribution of mean quantile normalized TSI (tissue specificity index) values of all miRNAs profiled by *human miRNA tissue atlas*[31]. **b** The heatmap represents the expression values of the identified exosomal miRNAs across all tissues, averaged over two bodies. Expression values were quantile normalized and z-transformed; the profile of *miR-323b-3p* was not available in the repository and excluded. TSI values (averaged across two bodies) are shown next to the miRNA identifiers. **c** Enrichment analysis of 15 exosomal miRNAs identified to be associated with MS activity; dashed line shows the significant cut-off of p value = 0.01; grey bars indicate insignificance based on the selected cut-off

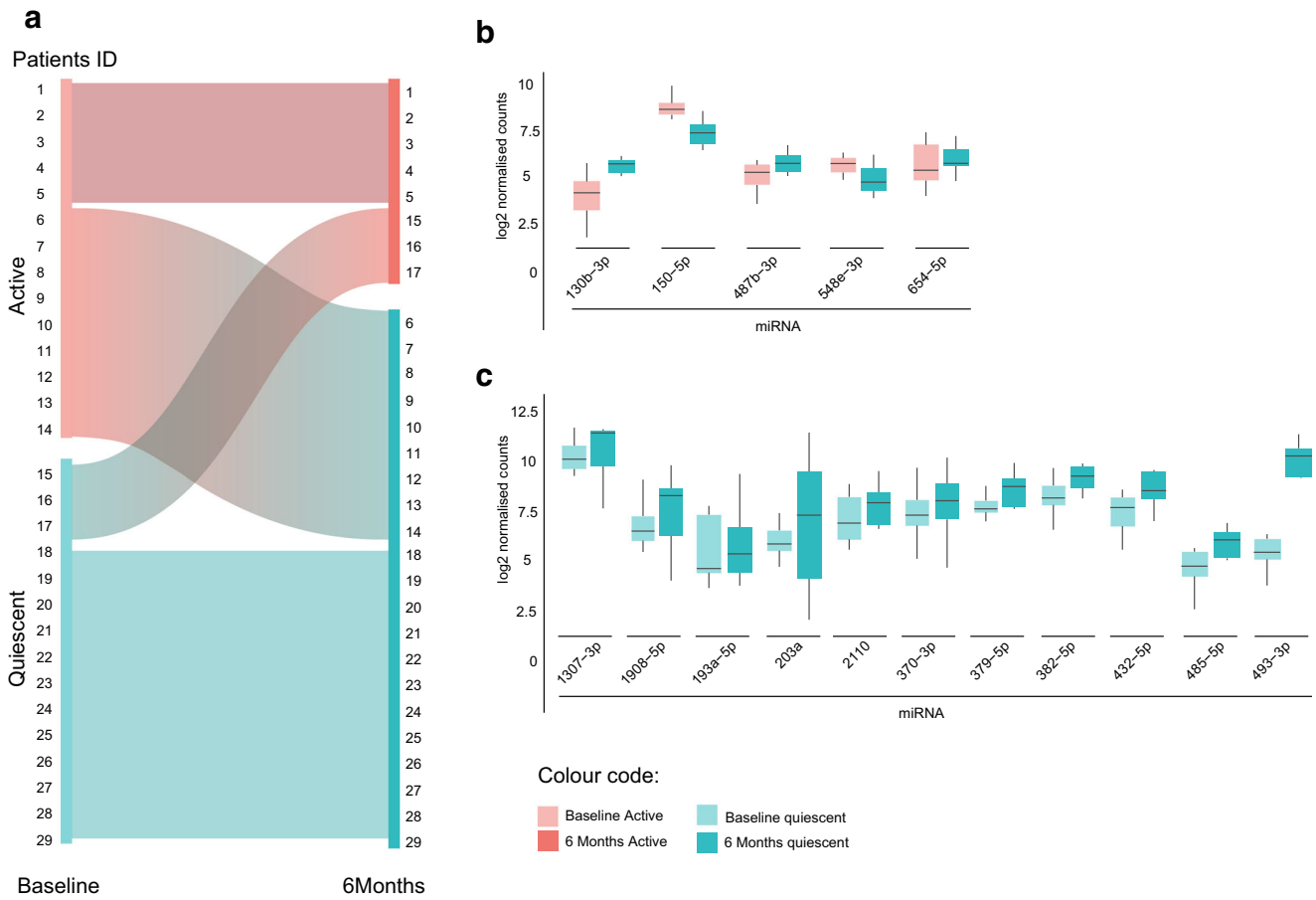

Fig. 4 MiRNA dysregulation associated with drug response. MS disease activity, based on Gd-MRI scan results, was monitored at baseline (15 quiescent and 14 active) and 6 months after fingolimod treatment. Twelve out of 15 quiescent patients remained stable (stable responders), and nine out of 14 active patients at baseline became quiescent after 6 months of treatment (positive responders). Differentially expressed miRNAs were then identified based on the adopted criteria |log2 (fold change)| > 1 and p value < 0.05. Eleven and five differentially expressed miRNA in stable and positive responder groups were respectively identified, as shown in the box-and-whisker plots

The values range from 0 to 1, with scores close to 0 representing miRNAs expressed in many or all tissues (i.e., housekeepers) and scores close to 1 implying that miRNAs expressed in only one specific tissue. Quantile-normalized miRNA expression profiles across all tissues were downloaded from the online repository (https://ccb-web.cs.uni-saarland.de/tissueatlas); expression values on similar tissues were averaged across two bodies. Similarly, mean normalized TSI scores for each miRNA were obtained from the same repository. Figure 3a shows the distribution of TSI values across all profiled miRNAs; ~ 10% of miRNAs have TSI ≥ 0.85 defined to be highly tissue-specific.

Of 15 exosomal miRNAs markers identified in this study, *miR-323b-3p* was not profiled in the repository and thus excluded. Among the remaining miRNAs, *miR-127-3p*, *-375*, *-379-5p* and *-411-5p* were predominantly expressed in central nervous system, brain in particular—i.e. TSI > 0.86; *miR-382-5p*, *-485-5p*, and *-889-3p* were also shown relatively high brain-specificity—i.e. TSI > 0.77 (Fig. 3b).

Additionally, we performed miRNA enrichment analysis on target genes inversely regulated in MS brain lesions to tease out exosomal miRNAs that are likely to be functionally active in brain. We performed right-sided Fisher's exact test on differentially expressed targets and identified statistically enriched miRNAs (adjusted p value < 0.01). Interestingly, we have observed that all brain-specific miRNAs were also highly enriched using an independent statistical analysis (Fig. 3c) which further corroborate their active function and reveal their potential targets.

Serum Exosome MiRNA Alterations in Response to Fingolimod Therapy

At baseline, 48% (14 of 29) of RRMS patients had objective evidence of active disease (defined by the presence of Gd enhancing lesions on MRI); 6 months post-treatment with fingolimod, the proportion of patients with active disease fell to 28% (8 of 29; Fig. 4a). To explore longitudinal alterations

Table 3 MicroRNAs with significant longitudinal alterations (p value < 0.05 and $|\log2 \text{ fold change}| > 1$) in patients stably or positively responded to fingolimod therapy as defined by Gd enhancing lesions on MRI

MicroRNA[a]	Log_2 FC	Average expression[b]	p value
150-5p	− 1.48	7.98	0.0012
130b-3p	1.53	4.57	0.0043
548e-3p	− 1.14	5.14	0.0059
487b-3p	1.11	5.24	0.0275
654-5p	1.11	5.79	0.0475
432-5p	1.26	8.04	0.004
485-5p	1.17	5.35	0.006
2110	1.07	7.53	0.0071
1307-3p	1.00	10.43	0.0081
382-5p	1.09	8.79	0.0116
370-3p	1.06	7.72	0.0121
379-5p	1.01	8.18	0.0125
493-3p	1.01	6.08	0.0135
1908-5p	1.32	7.15	0.0174
193a-5p	1.05	5.73	0.0422
203a	2.02	6.5	0.0445

FC fold change

[a] The line separates miRNAs differentially expressed in positive (top) and stable responders (bottom)

[b] Log_2 reads per million

of exosomal miRNAs in response to fingolimod therapy, miRNA profiles of treatment responders were compared at baseline versus 6-month follow-up; *stable responders* (i.e., patients with no evidence of Gd-enhancing lesions at both baseline and 6-month follow-up) and *positive responders* (i.e., patients showing active Gd-enhancing lesions at baseline and no enhancing lesions after 6 months of treatment) were separately considered for differential expression comparison to improve within-group homogeneity. The latter comparison revealed that the expression levels of two miRNAs (*miR-150-5p* and *-548e-3p*) decreased with treatment, while the expression of *miR-130b-3p*, *-654-5p*, *-487b-3p* increased after treatment. Additionally, 11 miRNAs (*miR-203a*, *-193a-5p*, *-379-5p*, *-370-3p*, *-382-5p*, *-493-3p*, *-432-5p*, *-485-5p*, *-2110*, *-1307-3p*, *-1908-5p*) were significantly upregulated in stable responders after 6 months of treatment (Table 3; Fig. 4b).

All patients remained on fingolimod and were clinically assessed at 12 months following treatment initiation. While 72% of patients had no evidence of Gd-enhancing lesions on MRI at 6 months post-treatment, this proportion increased to 90% after 12 months of treatment. Overall, the anti-inflammatory effect of fingolimod therapy was evident after 6 months of treatment and was persistent to the 12-month time point in patients with treatment response, except for patient 13 who demonstrated Gd-enhancing lesions on brain MRI after 12 months of fingolimod treatment. Of the eight patients who had not responded to treatment at the 6-month follow-up, five demonstrated a response to fingolimod after 12 months of treatment. Subsequently, while an increased treatment course improved the outcome as defined by fewer MS cases demonstrating Gd-enhancing lesions on MRI, 6 months of therapy was considered sufficient to reflect the effect of fingolimod and the miRNA regulatory changes associated with treatment efficacy. This observation is further corroborated by a prior study on the effect of fingolimod on circulating miRNAs indicating that the miRNA expression profile significantly changes after 6 months of therapy [11], and by the results of a pivotal placebo-controlled trial of fingolimod in RRMS, which showed a beneficial effect on MRI-related outcomes by 6 months [32].

Functional Roles of MiRNAs Altered in Response to Fingolimod Treatment

Next, pathways associated with identified miRNAs were determined to further explore how these pharmacogenomic miRNAs are potentially involved in fingolimod action and metabolism. Accordingly, for each differentially expressed miRNA, target genes from multiple miRNA-target interaction databases were retrieved if experimentally validated or computationally predicted by two or more datasets (Fig. 5a). Pathway enrichment analysis was then performed using KEGG [33] and Reactome [34] databases comprising 860 pathways in total, to identify pathways overrepresented by targets of each miRNA (Fig. 5b). Pathways enriched by multiple miRNAs are more robustly associated with drug-induced perturbations. Subsequently, pathways were sorted by total number of associated miRNAs and the top 10% of pathways were chosen (Fig. 5c). Selected pathways were then sorted under six general categories: *immune system*, *nervous system*, *signal transduction*, *lipid metabolism* and *signal transduction*, by consulting Reactome and KEGG pathway hierarchies (Fig. 5d). Multiple pathways relevant to the pathophysiology of MS and therapeutic targets were frequently enriched by miRNAs whose expression levels were altered in response to therapy, suggesting additional mechanisms of fingolimod action (*c.f.* "Discussion"). Moreover, miR-*130b-3p*, *-150-5p*, and *-2110*, directly target sphingosine 1-phosphate (S1P), enriching known fingolimod-induced pathways such as *sphingolipid metabolism* [35] and *sphingolipid* de novo *biosynthesis* [36].

Discussion

There is a growing body of evidence that highlights the regulatory role of miRNAs in the pathogenesis of MS and their potential therapeutic implications [8, 11–13, 15, 37–43]. Small RNA sequencing, unlike microarray or other targeted

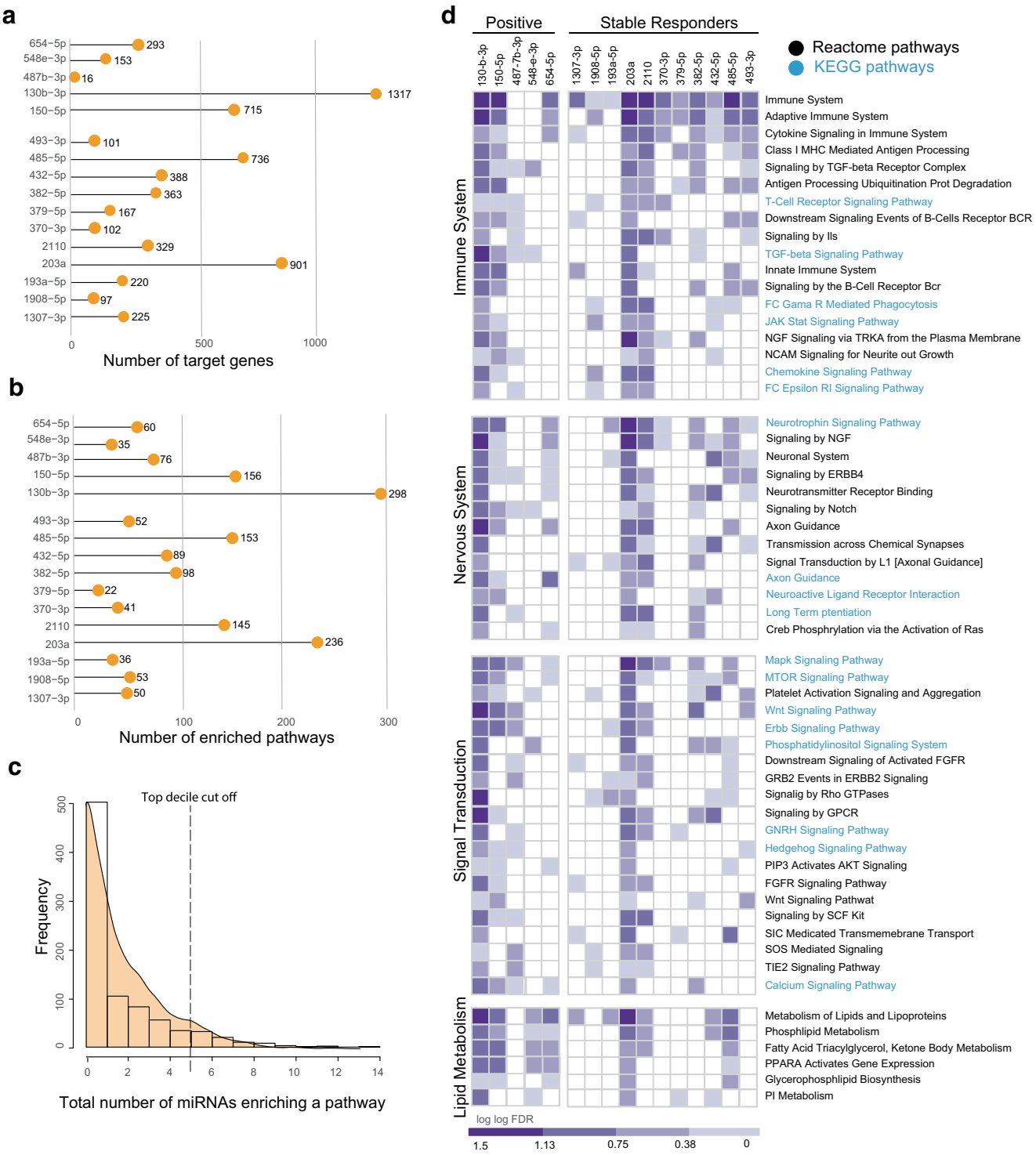

Fig. 5 Functional role of dysregulated pharmacogenomic miRNAs. **a** The bar plot shows the total number of genes targeted by each of dysregulated miRNAs. **b** Pathway enrichment analysis was performed to identify overrepresented pathways by targets of each miRNA; the bar plot shows the total number of pathways enriched by targets of each dysregulated miRNA. **c** Pathways enriched by multiple miRNAs suggest more robust association with drug-induced perturbation. The histogram shows the distribution of the total number of miRNAs enriching a pathway. The top 10% of robust pathways enriched by five or more miRNAs were chosen. **d** Selected pathways (top decile cut off) were classified into four MS-relevant categories of immune system, nervous system, signal transduction, lipid metabolism, diseases, and cell cycle by consulting Reactome (black) and KEGG (blue) hierarchies

technologies, allows an unbiased assessment of the total miRNA pool in any given sample. Here, we used this technique to profile the miRNAs encapsulated within circulating exosomes of RRMS patients in a search for biomarkers of response to a common therapy. Such an approach is arguably superior to profiling miRNAs in whole serum, particularly for MS, as exosomes are shed from affected cells in the CNS, and readily cross the blood-brain barrier into the circulation.

MS-associated miRNA biomarkers were identified as those differentially expressed in Gd-MRI-based active versus quiescent RRMS patients. Machine learning approaches on differentially expressed miRNAs were used to examine their individual and collective predictive powers in discriminating disease activity. While some differentially expressed miRNAs have been previously identified as circulating markers in MS or other immunological or nervous system diseases—e.g., *miR-375* in primary progressive MS[44], *miR-1246* in an active phase of systemic lupus erythematosus[45] and *miR-19b-3p* in Alzheimer's disease[46]—the majority of them are novel. This likely reflects the unique expression profile of miRNAs within exosomes versus free circulating miRNAs.

An integrative bioinformatics pipeline was developed to investigate the functional role of identified miRNA markers by constructing a network of miRNA-target gene interactions and improving prediction specificity by considering target genes associated with MS disease activity. Within the over-represented biological processes, we found canonical immune-associated pathways such as *positive regulation of interleukin 1 Beta production*, which plays a role in MS-associated neurodegenerative damage and clinical progression [47]. Two other conspicuous enriched immune-associated pathways were *leukocyte activation* and *regulation of type I interferon production*. In a healthy CNS, leukocytes have limited access to the brain and spinal cord, whereas in several neurological diseases, including MS, leukocytes infiltrate from the periphery into the CNS resulting in inflammation [48]. Conversely, type 1 interferon is an immunomodulatory cytokine with anti-inflammatory effects via controlling interleukin I[49]. Tissue specificity of the signature miRNAs was investigated to discern those originated from brain as potential direct suppressors of targets downregulated in MS brain lesions. Several MS-associated miRNA biomarkers identified in this study were predominantly expressed in brain and spinal cord, among them *miR-375* holds the highest specificity (TSI = 0.96) which corroborates previous observations (e.g., [50]).

Investigating the role of miRNAs in the pathogenesis of MS and identifying miRNA-based pharmacogenomic markers of treatment response is an active field of research [11, 12, 15, 37, 38, 43]. Hence, identified exosomal miRNAs associated with fingolimod treatment efficacy as those miRNAs longitudinally changed in treatment responders, i.e., patients whose disease remained inactive or become inactive after 6 months of treatment. Altered expression and the function of some of the predicted miRNAs have been previously reported in studies of the peripheral blood of MS patients. The expression of *miR-130b* and *miR-203* was shown to be altered in B cells from peripheral blood samples of RRMS patients [51]. In the current study, these two miRNAs target the highest number of genes over-representing multiple pathways involved in immune system, nervous system, lipid metabolism as well as critical signal transduction. The dysregulation of *miR-150* in the B cells of peripheral blood samples of MS patients following treatment with natalizumab has also been reported [51]. Additionally, the expression of *miR-150* was downregulated in T cell [52] and peripheral blood mononuclear cells (PBMC) of MS patients compared to healthy controls [53]. The altered expression of *miR-193a-5p* has been previously reported in PBMC of RRMS patients after 6 months of interferon-beta therapy [14].

Next, pathways consistently overrepresented by targets of multiple miRNAs associated with treatment response were identified. Multiple pathways pivotal in MS pathogenesis and relevant to fingolimod mechanisms have been enriched. For instance, T cell development and function critically influence disease pathogenesis and treatment response [54]. Additionally, the *TGFβ signalling pathway* regulates the differentiation of naïve CD4 T cells into regulatory T cells, and a reduction in this signalling pathway results in a fewer number of regulatory T cells being observed in MS patients [55, 56]. Our results indicate that upregulated miRNAs in response to fingolimod perturb the TGFβ signalling pathway, which in turn may result in a reduced susceptibility to MS disease activity. Another predicted pathway, the *JAK-STAT pathway*, has an indirect effect on interleukin-7 expression (IL-7) which is an important cytokine for the regulation of B cell and T cell development and is overexpressed in MS brain lesions [57]. Another interesting and important pathway is the *Wnt signalling pathway*, enriched by targets of seven miRNAs in this current study. The Wnt pathway modulates the immune response and is involved in the process of remyelination by controlling the balance between immune tolerance/inflammation and neuronal survival/neurodegeneration in MS [58].

In summary, our results demonstrate that serum exosomal miRNAs are altered by disease activity and after treatment with fingolimod. We identified miRNAs specifically altered in treatment responders and predicted their impact on a variety of pivotal regulatory pathways, furthering our understanding of MS immunopathogenesis and the action and metabolism of fingolimod. Importantly, this work suggests that exosomal miRNA profiles have the potential to be utilized in MS clinical practice as biomarkers of disease activity and treatment response to drive personalized therapeutic choices. Longitudinal analysis of larger cohorts of RRMS patients with

diverse patterns of response to fingolimod therapy are required to confirm our findings.

Acknowledgements We would like to acknowledge and thank the patients who were involved in the study. We would like to thank the University of Sydney MS Clinical Trials staff for their assistance with venepuncture, serum preparation and storage and general study facilitation.

Author Contributions MHB, HNB, and MEB conceptualized and designed the study and provided critical review of the manuscript. HNB collected patients' specimens, clinical and MRI information. SE and CW were involved in technical work for data acquisition; SE performed exosome purification and RNA extraction. FV developed the machine learning and bioinformatics pipelines. FV and SE analysed the data and generated the results. All the authors were involved in data interpretation. FV, SE and CMS drafted the manuscript and prepared the figures. All the authors revised and approved the final version.

Funding information This project was partly funded by Novartis Australia.

Data Availability The RNA-seq profile of exosomal miRNAs produced in this study is available at GEO repository with accession number **GSE140106**.

Compliance with Ethical Standards

Ethical approval for the study was obtained from the University of Sydney Human Research Ethics Committee (2014/054).

Conflict of Interest Heidi N Beadnall has received honoraria for presentations and advisory boards and has received educational travel support from Novartis, whom markets Gilenya®. Michael Barnett has received institutional support for research, speaking and/or participation in advisory boards for Biogen, Merck, Novartis, Roche and Sanofi Genzyme. He is a research consultant at Medical Safety Systems and research director for the Sydney Neuroimaging Analysis Centre. Michael E Buckland has received honoraria for presentations from Novartis and Biogen.

References

1. Milo R, Miller A (2014) Revised diagnostic criteria of multiple sclerosis. Autoimmun Rev 13(4–5):518–524
2. Thompson AJ et al (2018) Multiple sclerosis. Lancet 391(10130): 14
3. Cree BA, Mares J, Hartung H-P (2019) Current therapeutic landscape in multiple sclerosis: an evolving treatment paradigm. 32(3): 365–377
4. Ciccarelli OJTLN (2019) Multiple sclerosis in 2018: new therapies and biomarkers. 18(1):10–12
5. English C, Aloi JJ (2015) New FDA-approved disease-modifying therapies for multiple sclerosis. Clin Ther 37(4):691–715
6. Fonseca J (2015) Fingolimod real world experience: efficacy and safety in clinical practice
7. Chun J et al (2019) Fingolimod: lessons learned and new opportunities for treating multiple sclerosis and other disorders. 59:149–170
8. Ebrahimkhani S et al (2017) Exosomal microRNA signatures in multiple sclerosis reflect disease status. Sci Rep 7(1):14293
9. De Felice B et al (2014) Small non-coding RNA signature in multiple sclerosis patients after treatment with interferon-β. BMC Med Genet 7(1):26
10. Junker A, Hohlfeld R, Meinl E (2011) The emerging role of microRNAs in multiple sclerosis. Nat Rev Neurol 7(1):56–59
11. Fenoglio C et al (2016) Effect of fingolimod treatment on circulating miR-15b, miR23a and miR-223 levels in patients with multiple sclerosis. J Neuroimmunol 299:81–83
12. Waschbisch A et al (2011) Glatiramer acetate treatment normalizes deregulated microRNA expression in relapsing remitting multiple sclerosis. PLoS One 6(9):e24604
13. Gandhi R (2015) miRNA in multiple sclerosis: search for novel biomarkers. Mult Scler 21(9):1095–1103
14. Hecker M et al (2013) MicroRNA expression changes during interferon-beta treatment in the peripheral blood of multiple sclerosis patients. Int J Mol Sci 14(8):16087–16110
15. Ingwersen J et al (2015) Natalizumab restores aberrant miRNA expression profile in multiple sclerosis and reveals a critical role for miR-20b. Ann Clin Transl Neurol 2(1):43–55
16. Polman CH et al (2011) Diagnostic criteria for multiple sclerosis: 2010 revisions to the McDonald criteria. Ann Neurol 69(2):292–302
17. Kurtzke JF (1983) Rating neurologic impairment in multiple sclerosis: an expanded disability status scale (EDSS). Neurology 33(11):1444–1444
18. Kaunzner UW, Gauthier SA (2017) MRI in the assessment and monitoring of multiple sclerosis: an update on best practice. Ther Adv Neurol Disord 10(6):247–261
19. Giorgio A, De Stefano N (2018) Effective utilization of MRI in the diagnosis and management of multiple sclerosis. Neurol Clin 36(1): 27–34
20. Filippi M, Preziosa P, Rocca MA (2014) Magnetic resonance outcome measures in multiple sclerosis trials: time to rethink? Curr Opin Neurol 27(3):290–299
21. Filippi M et al (2019) Association between pathological and MRI findings in multiple sclerosis. 18(2):198–210
22. Lotvall J et al (2014) Minimal experimental requirements for definition of extracellular vesicles and their functions: a position statement from the International Society for Extracellular Vesicles. J Extracell Vesicles 3:26913
23. Charity W, Law YC, Shi W, Smyth GK (2014) voom: precision weights unlock linear model analysis tools for RNA-seq read counts. Genome Biol 15:R29
24. Liu R et al (2015) Why weight? Modelling sample and observational level variability improves power in RNA-seq analyses. Nucleic Acids Res 43(15):e97
25. Smyth GK (2004) Linear models and empirical bayes methods for assessing differential expression in microarray experiments. Stat Appl Genet Mol Biol 3:3
26. DeLong ER, DeLong DM, Clarke-Pearson DL (1988) Comparing the areas under two or more correlated receiver operating characteristic curves: a nonparametric approach. Biometrics:837–845
27. Tukey JW (1977) Exploratory data analysis. Vol. 2: Reading, Mass
28. Breiman L (2001) Random forests. Mach Learn 45(1):5–32
29. Liberzon A et al (2015) The molecular signatures database hallmark gene set collection. Cell Syst 1(6):417–425
30. Ru Y et al (2014) The multiMiR R package and database: integration of microRNA–target interactions along with their disease and drug associations. Nucleic Acids Res 42(17):e133–e133
31. Ludwig N et al (2016) Distribution of miRNA expression across human tissues. 44(8):3865–3877
32. Kappos L et al (2010) A placebo-controlled trial of oral fingolimod in relapsing multiple sclerosis. N Engl J Med 362(5):387–401

33. Kanehisa M et al (2016) KEGG: new perspectives on genomes, pathways, diseases and drugs. Nucleic Acids Res 45(D1):D353–D361
34. Fabregat A et al (2017) The reactome pathway knowledgebase. Nucleic Acids Res 46(D1):D649–D655
35. Prager B, Spampinato SF, Ransohoff RM (2015) Sphingosine 1-phosphate signalling at the blood-brain barrier. Trends Mol Med 21(6):354–363
36. Pistono C et al (2017) What's new about oral treatments in multiple sclerosis? Immunogenetics still under question. Pharmacol Res 120:279–293
37. Meira M et al (2014) Unravelling natalizumab effects on deregulated miR-17 expression in CD4+ T cells of patients with relapsing-remitting multiple sclerosis. J Immunol Res 2014: 897249
38. Muñoz-Culla M, Irizar H, Castillo-Triviño T, Sáenz-Cuesta M, Sepúlveda L, Lopetegi I, de Munain AL, Olascoaga J et al (2014) Blood miRNA expression pattern is a possible risk marker for natalizumab-associated progressive multifocal leukoencephalopathy in multiple sclerosis patients. Mult Scler J 20(14):1851–1859
39. Guerau-de-Arellano M, Lovett-Racke AE, Racke MK (2010) miRNAs in multiple sclerosis: regulating the regulators. J Neuroimmunol 229(1–2):3–4
40. Yang Q, Pan W, Qian L (2017) Identification of the miRNA-mRNA regulatory network in multiple sclerosis. Neurol Res 39(2):142–151
41. Fenoglio C et al (2013) Decreased circulating miRNA levels in patients with primary progressive multiple sclerosis. Mult Scler J 19(14):1938–1942
42. De Santis G et al (2010) Altered miRNA expression in T regulatory cells in course of multiple sclerosis. J Neuroimmunol 226(1–2): 165–171
43. Zinger A et al (2016) Plasma levels of endothelial and B cell-derived microparticles are restored by fingolimod treatment in multiple sclerosis patients. Mult Scler J 22(14):1883–1887
44. Vistbakka J et al (2017) Circulating microRNAs as biomarkers in progressive multiple sclerosis. Mult Scler J 23(3):403–412
45. Husakova M (2016) MicroRNAs in the key events of systemic lupus erythematosus pathogenesis. Biomed Pap Med Fac Univ Palacky Olomouc Czech Repub 160(3):327–342
46. Wu Y et al (2017) Lower serum levels of miR-29c-3p and miR-19b-3p as Biomarkers for Alzheimer's disease. Tohoku J Exp Med 242(2):129–136
47. Rossi S et al (2014) Interleukin-1β causes excitotoxic neurodegeneration and multiple sclerosis disease progression by activating the apoptotic protein p53. Mol Neurodegener 9(1):56
48. Rawji KS, Yong VW (2013) The benefits and detriments of macrophages/microglia in models of multiple sclerosis. Clin Dev Immunol 2013:948976
49. Guarda G et al (2011) Type I interferon inhibits interleukin-1 production and inflammasome activation. Immunity 34(2):213–223
50. Bhinge A et al (2016) MiR-375 is essential for human spinal motor neuron development and may be involved in motor neuron degeneration. 34(1):124–134
51. Sievers C et al (2012) Altered microRNA expression in B lymphocytes in multiple sclerosis. Clin Immunol 144(1):70–79
52. Jernås M, Malmeström C, Axelsson M, Nookaew I, Wadenvik H, Lycke J, Olsson B (2013) MicroRNA regulate immune pathways in T-cells in multiple sclerosis (MS). BMC Immunol 14(32)
53. Martinelli-Boneschi F et al (2012) MicroRNA and mRNA expression profile screening in multiple sclerosis patients to unravel novel pathogenic steps and identify potential biomarkers. Neurosci Lett 508(1):4–8
54. Venken K et al (2008) Natural naive CD4+ CD25+ CD127low regulatory T cell (Treg) development and function are disturbed in multiple sclerosis patients: recovery of memory Treg homeostasis during disease progression. J Immunol 180(9):6411–6420
55. Severin ME et al (2016) MicroRNAs targeting TGFbeta signalling underlie the regulatory T cell defect in multiple sclerosis. Brain 139(Pt 6):1747–1761
56. Petrocca F, Vecchione A, Croce CM (2008) Emerging role of miR-106b-25/miR-17-92 clusters in the control of transforming growth factor beta signalling. Cancer Res 68(20):8191–8194
57. Jana M et al (2014) Interleukin-12 (IL-12), but not IL-23, induces the expression of IL-7 in microglia and macrophages: implications for multiple sclerosis. Immunology 141(4):549–563
58. Libro R, Bramanti P, Mazzon E (2016) The role of the Wnt canonical signalling in neurodegenerative diseases. Life Sci 158:78–88